

A comparison of models for calculating nuclear magnetic resonance shielding tensors

James R. Cheeseman, Gary W. Trucks, Todd A. Keith, and Michael J. Frisch
Lorentzian, Inc., 140 Washington Avenue, North Haven, Connecticut 06473

(Received 1 December 1995; accepted 5 January 1996)

The direct (recomputation of two-electron integrals) implementation of the gauge-including atomic orbital (GIAO) and the CSGT (continuous set of gauge transformations) methods for calculating nuclear magnetic shielding tensors at both the Hartree-Fock and density functional levels of theory are presented. Isotropic ^{13}C , ^{15}N , and ^{17}O magnetic shielding constants for several molecules, including taxol ($\text{C}_{47}\text{H}_{51}\text{NO}_{14}$ using 1032 basis functions) are reported. Shielding tensor components determined using the GIAO and CSGT methods are found to converge to the same value at sufficiently large basis sets; however, GIAO shielding tensor components for atoms other than carbon are found to converge faster with respect to basis set size than those determined using the CSGT method for both Hartree-Fock and DFT. For molecules where electron correlation effects are significant, shielding constants determined using (gradient-corrected) pure DFT or hybrid methods (including a mixture of Hartree-Fock exchange and DFT exchange-correlation) are closer to experiment than those determined at the Hartree-Fock level of theory. For the series of molecules studied here, the RMS error for ^{13}C chemical shifts relative to TMS determined using the B3LYP hybrid functional with the 6-311+G(2*d*,*p*) basis is nearly three times smaller than the RMS error for shifts determined using Hartree-Fock at this same basis. Hartree-Fock ^{13}C chemical shifts calculated using the 6-31G* basis set give nearly the same RMS error as compared to experiment as chemical shifts obtained using Hartree-Fock with the bigger 6-311+G(2*d*,*p*) basis set for the range of molecules studied here. The RMS error for chemical shifts relative to TMS calculated at the Hartree-Fock 6-31G* level of theory for taxol ($\text{C}_{47}\text{H}_{51}\text{NO}_{14}$) is 6.4 ppm, indicating that for large systems, this level of theory is sufficient to determine accurate ^{13}C chemical shifts. © 1996 American Institute of Physics. [S0021-9606(96)01914-X]

I. INTRODUCTION

A number of methods have been developed for the calculation of molecular second-order magnetic response properties. It is generally accepted that accurate prediction of these properties within the finite basis approximation, requires gauge-invariant procedures.^{1,2} This paper will focus on predicting NMR shielding tensors using two of these procedures, namely GIAO and CSGT at both the Hartree-Fock and DFT levels of theory, which achieve “gauge-invariance” in different ways. The GIAO method, which uses basis functions that have an explicit field dependence,³ was first adopted for quantum chemical NMR shift calculations by Ditchfield.⁴ More recent implementations at the Hartree-Fock level include those by Pulay⁵ and Gauss.¹ The CSGT method, developed by Keith and Bader,² achieves gauge-invariance by performing a continuous set of gauge transformations, one for each point in real space, obtaining an accurate description of the current density from which the shielding tensors can be determined.

Gauge-invariant Hartree-Fock (at sufficiently large basis sets) methods give ^{13}C shielding results which are close to experiment for most hydrocarbon molecules and other molecules where electron correlation effects are relatively small. For molecules with multiple bonds, electron correlation contributions become more significant and these effects need to be included in order to obtain accurate shielding tensors, especially for other nuclei such as ^{15}N and ^{17}O .¹ In order to

include these electron correlation contributions, Gauss has recently developed the GIAO-MP2¹ and GIAO-CCSD⁶ methods which provide shielding constants that are consistently in close agreement with experiment.

Density functional theory has emerged in recent years as a promising alternative to conventional *ab initio* methods in quantum chemistry. DFT has been shown to be successful in predicting various molecular properties, often giving results of a quality comparable or even better than MP2 for a cost that is on the same order as Hartree-Fock, substantially less than that of traditional correlation techniques. It therefore seems reasonable to investigate in detail how well DFT predicts magnetic response properties, in particular shielding tensors.

Vignale and co-workers,⁷ in their study of magnetic fields and DFT, proposed a term for the current dependency of the exchange-correlation functional. Malkin and co-workers⁸ have previously implemented methods for calculating DFT magnetic properties within the individual gauge for localized orbitals (IGLO)⁹ framework using current-dependent functionals. Friedrich *et al.*¹⁰ were the first to combine the GIAO method with DFT, however their study was limited by their use of the X_α exchange-correlation functional and of minimal basis sets. Schreckenbach and Ziegler¹¹ have recently implemented the GIAO method at the DFT level of theory and examined one functional (LDA/NL) using relatively small basis sets for a small

number of molecules. In addition, their implementation employs Slater type orbitals as basis functions, as opposed to the more common Gaussian type orbitals used in our implementation here. The results they obtained are encouraging and indicate a need to examine other functionals, including hybrid functionals, for a larger range of systems.

In this paper we discuss the implementation of the GIAO and CSGT methods for calculating NMR shielding tensors at both the Hartree-Fock and DFT levels of theory, using functionals which do not include a specific magnetic field dependent term, but which have yielded good accuracy for other chemical properties.^{12,13} The convergence of NMR isotropic shielding constants with respect to basis set using the CSGT and GIAO methods is examined. Several functionals, including hybrid functionals, are investigated in their ability to predict NMR ¹³C, ¹⁵N, and ¹⁷O chemical shifts using GIAO's and a relatively large basis set which is known to be sufficient to predict accurate MP2 chemical shifts. In addition, absolute shielding constants for CO, N₂, and NNO, where electron correlation contributions are large, are presented for these functionals using a very large basis set. We compare methods for calculating accurate NMR chemical shifts for large molecules, especially for ¹³C, while examining the trade-off between accuracy and cost. Our test set is composed of a range of molecules which have different environments for the nuclei of interest. These include systems with single and multiple bonds, molecules where electron correlation effects are significant such as the benzenium ion,¹⁴ phenonium ion,¹⁴ and C₂B₃H₅.¹⁵ In addition, bicyclobutane and [1.1.1.]propellane are included as examples of strained ring systems. Finally, ¹³C chemical shifts for the taxol molecule (1037 basis functions) are reported as an example large system.

II. THEORY AND IMPLEMENTATION

The nuclear magnetic shielding tensor is expressed as the mixed second derivative of the energy with respect to the external magnetic field, \vec{B} , and the magnetic moment of nucleus N , m_N .

$$\sigma_{ji}^N = \frac{\partial^2 \mathcal{E}}{\partial B_i \partial m_{N_j}}, \quad (1)$$

where i and j are the components of the external magnetic field and induced magnetic moment, respectively. The Kohn-Sham (KS) formulation¹⁶ of DFT is closely analogous to Hartree-Fock (HF) theory in that a set of molecular orbitals is derived from an effective one-electron potential via a self-consistent procedure. Considering SCF theory in general, the SCF energy and Fock matrix are

$$\mathcal{E} = \langle \mathbf{hP} \rangle + \frac{1}{2} \langle \mathbf{PG}_{2e}(\mathbf{P}) \rangle + E_{\text{XC}} + \mathcal{V}, \quad (2)$$

$$\mathbf{F} = \frac{\partial \mathcal{E}}{\partial \mathbf{P}} = \mathbf{h} + \mathbf{G}_{2e}(\mathbf{P}) + \mathbf{G}_{\text{XC}} = \mathbf{h} + \mathbf{G}, \quad (3)$$

where \mathbf{P} is the density matrix, \mathbf{h} is the one-electron Hamiltonian and \mathcal{V} is the nuclear repulsion energy and

$$\mathbf{G}_{2e}(\mathbf{P})_{\mu\nu} = \sum_{\lambda\sigma} \mathbf{P}_{\lambda\sigma} (\mu\lambda || \nu\sigma), \quad (4)$$

where $(\mu\lambda || \nu\sigma)$ is the antisymmetrized two-electron integral over spin orbitals $\chi_\mu, \chi_\nu, \chi_\lambda, \chi_\sigma$ which includes a coefficient for Hartree-Fock exchange, C_{HFX} , as follows (this definition is assumed throughout)

$$(\mu\lambda || \nu\sigma) = \int \chi_\mu^*(1) \chi_\lambda^*(2) \frac{1}{r_{12}} [\chi_\nu(1) \chi_\sigma(2) - C_{\text{HFX}} \chi_\sigma(1) \chi_\nu(2)] d\tau_1 d\tau_2. \quad (5)$$

The exchange-correlation energy is

$$E_{\text{XC}} = \int f(\rho_\alpha, \rho_\beta, \gamma_{\alpha\alpha}, \gamma_{\alpha\beta}, \gamma_{\beta\beta}) d\vec{r}, \quad (6)$$

where α and β refer to the spin components and f is a general first-order exchange-correlation functional and does not include an explicit magnetic field dependent term. The spin densities and density gradient invariants are given as follows:

$$\rho_\alpha = \sum_{\mu\nu} \mathbf{P}_{\mu\nu}^\alpha \chi_\mu \chi_\nu, \quad \gamma_{\alpha\alpha} = \nabla \rho_\alpha \cdot \nabla \rho_\alpha, \quad \gamma_{\alpha\beta} = \nabla \rho_\alpha \cdot \nabla \rho_\beta, \quad (7)$$

$$\nabla \rho_\alpha = \sum_{\mu\nu} \mathbf{P}^\alpha \nabla (\chi_\mu \chi_\nu),$$

and \mathbf{G}_{XC} , the exchange-correlation piece of \mathbf{F} is¹⁷

$$(\mathbf{G}_{\text{XC}}^\alpha)_{\mu\nu} = \int \left[\frac{\partial f}{\partial \rho_\alpha} \chi_\mu^* \chi_\nu + \left(2 \frac{\partial f}{\partial \gamma_{\alpha\alpha}} \nabla \rho_\alpha + \frac{\partial f}{\partial \gamma_{\alpha\beta}} \nabla \rho_\beta \right) \cdot \nabla (\chi_\mu^* \chi_\nu) \right] d\vec{r} \quad (8)$$

with a similar expression for $\mathbf{G}_{\text{XC}}^\beta$. The coefficient for Hartree-Fock exchange, C_{HFX} , in Eq. (5) is one for Hartree-Fock, zero for pure DFT and non-zero for hybrid methods. Similarly, $f=0$ for Hartree-Fock theory.

Using the notation where first and higher derivatives are denoted by superscripts specifying the variable(s) of differentiation, the expression for the shielding tensor for nucleus N becomes:

$$\sigma_{ji}^N = \frac{\partial^2 \mathcal{E}}{\partial B_i \partial m_{N_j}} = \langle \mathbf{h}^{(B_i, m_{N_j})} \mathbf{P} \rangle + \langle \mathbf{h}^{m_{N_j}} \mathbf{P}^{B_i} \rangle, \quad (9)$$

where the derivatives of the Hamiltonian are given by

$$\mathbf{h}_{\mu\nu}^{m_{N_j}} = \langle \chi_\mu | \hat{\mathbf{h}}^{m_{N_j}} | \chi_\nu \rangle; \quad \hat{\mathbf{h}}^{m_{N_j}} = -\frac{i}{c} \frac{[(\vec{r} - \vec{R}_N) \times \vec{\nabla}]_j}{|\vec{r} - \vec{R}_N|^3}, \quad (10)$$

$$\mathbf{h}_{\mu\nu}^{(B_i, m_{N_j})} = \langle \chi_\mu | \hat{\mathbf{h}}^{(B_i, m_{N_j})} | \chi_\nu \rangle; \quad \hat{\mathbf{h}}^{(B_i, m_{N_j})} = \frac{1}{2c^2} \frac{\vec{r} \cdot (\vec{r} - \vec{R}_N) \delta_{ij} - \vec{r}_i (\vec{r} - \vec{R}_N)_j}{|\vec{r} - \vec{R}_N|^3}. \quad (11)$$

In addition to the derivatives of the one-electron Hamiltonian, the calculation of the nuclear magnetic shielding tensor also requires the derivative of the density matrix with respect to the magnetic field, \mathbf{P}^{B_i} . This is obtained via solution of the coupled-perturbed (CP) equations for the appropriate perturbation. In order to discuss the magnetic field perturbation solution for hybrid methods such as B3LYP, which include a mixture of Hartree-Fock exchange and DFT exchange-correlation, a brief description of the CP equations will be presented here to illustrate the parallelism which exists between Hartree-Fock and DFT.

Separating \mathbf{P} into its occupied-occupied and virtual-occupied blocks, the CP equations for an external magnetic field perturbation B_i are

$$\mathbf{F}\mathbf{P}_{ov}^{B_i} - \mathbf{P}_{ov}^{B_i}\mathbf{F} - \mathbf{G}(\mathbf{P}_{ov}^{B_i} + \mathbf{P}_{vo}^{B_i})_{ov} = \mathbf{h}_{ov}^{B_i} + \mathbf{G}_{ov}^{B_i}(\mathbf{P})_{ov} - \mathbf{F}\mathbf{S}_{ov}^{B_i} + \mathbf{G}(\mathbf{S}_{oo}^{B_i})_{ov}, \quad (12)$$

$$\mathbf{P}_{oo}^{B_i} = -\mathbf{S}_{oo}^{B_i}, \quad \mathbf{P}_{vv}^{B_i} = \mathbf{0}, \quad (13)$$

where the subscripts oo and ov refer to the occupied-occupied and occupied-virtual blocks of the matrix, respectively. \mathbf{S} is the overlap matrix and $\mathbf{G}(\mathbf{X})$ (where \mathbf{X} is either $(\mathbf{P}_{ov}^{B_i} + \mathbf{P}_{vo}^{B_i})$ or $\mathbf{S}_{oo}^{B_i}$) is

$$\mathbf{G}(\mathbf{X})_{\mu\nu} = \sum_{\lambda\sigma} \mathbf{X}_{\lambda\sigma}(\mu\lambda||\nu\sigma), \quad (14)$$

where $(\mu\lambda||\nu\sigma)$ is as defined in Eq. (5). The term $\mathbf{G}^{B_i}(\mathbf{P})_{\mu\nu}$ which results from the derivative of the basis functions with respect to the field is

$$\mathbf{G}^{B_i}(\mathbf{P})_{\mu\nu} = \sum_{\lambda\sigma} \mathbf{P}_{\lambda\sigma}(\mu\lambda||\nu\sigma)^{B_i} + \mathbf{G}_{XC}^{B_i}. \quad (15)$$

Note that there is no corresponding exchange-correlation contribution to these equations because the standard functionals considered here depend only on $\rho(\vec{r})$ and its derivatives and not on the magnetic field explicitly. If C_{HFX} is taken to be one in Eq. (5) [with $f=0$ in Eqs. (8) and (21)], then the CPHF equations result from Eq. (12), while if C_{HFX} is zero, the CPKS equations are obtained. The efficient solution of Eq. (12) for \mathbf{P}_{ov}^x in the AO basis, for real perturbations has been discussed previously.^{17,18} For an imaginary perturbation, the coulomb contributions in both $\mathbf{G}(\mathbf{P}_{ov}^{B_i} + \mathbf{P}_{vo}^{B_i})_{ov}$ and $\mathbf{G}(\mathbf{S}_{oo}^{B_i})_{ov}$ [Eq. (14)] vanish leaving only the Hartree-Fock exchange contribution. Since ρ and its derivatives have only an *explicit* dependence upon the field (via the basis functions), the DFT exchange-correlation contribution to these two terms is zero and for pure DFT, the CPKS equations reduce to their uncoupled analog. For hybrid methods, which include a mixture of Hartree-Fock exchange and DFT exchange-correlation, only Hartree-Fock exchange is present in these two terms. As gauge-invariance is achieved in different ways, the GIAO and CSGT methods differ at this point in the formation of the right-hand side of Eq. (12).

A. GIAO method

The GIAO method^{1,3-5} for calculating magnetic properties uses the following explicit field-dependent basis functions.

$$\chi_{\mu}(\vec{B}) = \exp\left[-\frac{i}{2c}(\vec{B} \times \vec{R}_{\mu}) \cdot \vec{r}\right] \chi_{\mu}(\vec{0}), \quad (16)$$

where \vec{R}_{μ} is the position vector of basis function χ_{μ} and $\chi_{\mu}(\vec{0})$ denotes the usual field-independent basis functions. The derivative of a field-dependent basis function with respect to the magnetic field direction i is

$$\chi_{\mu}^{B_i} = -\frac{i}{2c}(\vec{R}_{\mu} \times \vec{r})_i \chi_{\mu}(\vec{0}). \quad (17)$$

Defining $\vec{R}_{\mu\nu} = \vec{R}_{\mu} - \vec{R}_{\nu}$, the derivative of the overlap \mathbf{S} and Hamiltonian \mathbf{h} matrices with respect to the external magnetic field in the AO basis are

$$\mathbf{S}_{\mu\nu}^{B_i} = \frac{i}{2c}(\vec{R}_{\mu\nu} \times \vec{r}) \langle \chi_{\mu} | \chi_{\nu} \rangle, \quad (18)$$

$$\begin{aligned} \mathbf{h}_{\mu\nu}^{B_i} &= \langle \chi_{\mu}^{B_i} | \hat{\mathbf{h}} | \chi_{\nu} \rangle + \langle \chi_{\mu} | \hat{\mathbf{h}}^{B_i} | \chi_{\nu} \rangle + \langle \chi_{\mu} | \hat{\mathbf{h}} | \chi_{\nu}^{B_i} \rangle \\ &= \frac{i}{2c}(\vec{R}_{\mu\nu} \times \langle \chi_{\mu} | \vec{r} | \chi_{\nu} \rangle - \langle \chi_{\mu} | \vec{r} \times \nabla | \chi_{\nu} \rangle \\ &\quad + \vec{R}_{\nu} \langle \chi_{\mu} | \nabla | \chi_{\nu} \rangle), \end{aligned} \quad (19)$$

where the derivative of the Hamiltonian operator is

$$\hat{\mathbf{h}}^{B_i} = -\frac{i}{2c}(\vec{r} \times \nabla)_i. \quad (20)$$

The term $\mathbf{G}_{XC}^{B_i}$ in Eq. (15), which results from the derivative of the field-dependent basis functions with respect to the field is

$$\begin{aligned} (\mathbf{G}_{XC}^{\alpha})_{\mu\nu}^{(B_i)} &= \int \left[\frac{\partial f}{\partial \rho_{\alpha}} (\chi_{\mu}^* \chi_{\nu})^{B_i} + \left(2 \frac{\partial f}{\partial \gamma_{\alpha\alpha}} \nabla \rho_{\alpha} \right. \right. \\ &\quad \left. \left. + \frac{\partial f}{\partial \gamma_{\alpha\beta}} \nabla \rho_{\beta} \right) \cdot \nabla (\chi_{\mu}^* \chi_{\nu})^{B_i} \right] d\vec{r}, \end{aligned} \quad (21)$$

where

$$(\chi_{\mu}^* \chi_{\nu})^{B_i} = \frac{i}{2c}(\vec{R}_{\mu\nu} \times \vec{r})_i \chi_{\mu}^* \chi_{\nu}, \quad (22)$$

and for the x component of the gradient,

$$\begin{aligned} \nabla_x (\chi_{\mu}^* \chi_{\nu})^{B_i} &= \frac{i}{2c}(\vec{R}_{\mu\nu} \times \vec{r})_i [(\nabla_x \chi_{\mu}^*) \chi_{\nu} + \chi_{\mu}^* (\nabla_x \chi_{\nu})] \\ &\quad + \frac{i}{2c} \chi_{\mu}^* \chi_{\nu} [(\vec{B} \times \vec{R}_{\mu\nu})_x^{B_i}]_{\vec{B}=0}. \end{aligned} \quad (23)$$

Three sets of Eq. (12) are then solved, one for each magnetic field direction.

B. CSGT methods

Alternatively, the nuclear magnetic shielding tensor can be expressed in terms of the induced first-order electronic current density $\mathbf{J}^{(1)}(\mathbf{r})$.

$$\sigma_{ji}^N = \frac{\partial^2 \mathcal{E}}{\partial B_i \partial m_{N_j}} = -\frac{1}{Bc} \int d\mathbf{r}_N [\mathbf{r}_N \times \mathbf{J}_i^{(1)}(\mathbf{r}) / r_N^3]_j. \quad (24)$$

The CSGT methods have been discussed in detail previously.^{2,19–21} While the GIAO method uses basis functions which depend on the field, the CSGT methods achieve gauge-invariance by accurately calculating the induced first-order electronic current density by performing a gauge transformation for each point in space. This is achieved by introducing the function $d(\vec{r})$ which is the shift in gauge origin and is defined to be a function of the real space field \vec{r} (not the electronic position vector fields \vec{r}_i) (discussed below). The expression for the first-order induced current density for a magnetic field applied along the x -axis using a continuous set of gauge transformations² is

$$\begin{aligned} \mathbf{J}^{(1)}(\vec{r}) = & \frac{1}{c} \sum_{i=1}^{n/2} B [\psi_i^* \hat{\mathbf{p}} \psi_i^{Lx} + \psi_i^{Lx*} \hat{\mathbf{p}} \psi_i - d_y(\vec{r}) (\psi_i^* \hat{\mathbf{p}} \psi_i^{pz} \\ & + \psi_i^{pz*} \hat{\mathbf{p}} \psi_i) + d_z(\vec{r}) (\psi_i^* \hat{\mathbf{p}} \psi_i^{py} + \psi_i^{py*} \hat{\mathbf{p}} \psi_i)] \\ & - \vec{B}(\vec{r} - d(\vec{r})) \rho(\vec{r}), \end{aligned} \quad (25)$$

where ρ is the electron density, $\hat{\mathbf{p}} = -i\nabla$ and the orbitals

$$\begin{aligned} \psi_i &= \sum_{\mu} c_{\mu i} \chi_{\mu}, \\ \psi_i^L &= \sum_{\mu} c_{\mu i}^L \chi_{\mu}, \\ \psi_i^p &= \sum_{\mu} c_{\mu i}^p \chi_{\mu}, \end{aligned} \quad (26)$$

where $c_{\mu i}$ are the molecular orbital expansion coefficients and the superscript L and p refer to the derivatives with respect to the angular momentum and linear momentum perturbations, respectively

$$\begin{aligned} \text{for } c_{\mu i}^L; \quad \hat{\mathbf{h}}^{B_i} &= -\frac{i}{2c} (\vec{r} \times \nabla)_i, \\ \text{for } c_{\mu i}^p; \quad \hat{\mathbf{h}}^{B_i} &= -\frac{i}{2c} \nabla_i. \end{aligned} \quad (27)$$

Since the basis functions do not depend upon the magnetic field, the only remaining term on the right-hand side of Eq. (12) is $\mathbf{h}_{\text{ov}}^{B_i}$. Six sets of these equations are then solved, three for the components of the angular momentum perturbation using any single gauge origin and three for the linear momentum perturbation resulting from any single shift in gauge origin. The shielding tensors are then obtained via Becke's²² multi-center numerical integration scheme, taking advantage of cutoffs.

1. $d(\vec{r})$ function

In the original implementation of the CSGT method by Keith and Bader,² an exponential function was used to shift the gauge origin. Here, the nuclear weight function used in Becke's algorithm²² for multi-center numerical integration is chosen for $d(\vec{r})$. Becke defines his nuclear weight function as follows

$$\mu_{ij} = \frac{r_i - r_j}{R_{ij}}, \quad (28)$$

where r_i and r_j denote distances to nuclei i and j , respectively, and R_{ij} is the inter-nuclear separation. The simplest possible function of μ satisfying the following constraints

$$\begin{aligned} f(-1) &= -1, \quad f(+1) = +1, \\ \frac{df}{d\mu}(-1) &= \frac{df}{d\mu}(+1) = 0, \end{aligned} \quad (29)$$

is a two-term polynomial

$$p(\mu) = \frac{3}{2}\mu - \frac{1}{2}\mu^3. \quad (30)$$

This simple polynomial, however, is not sharp enough so we iterate as follows

$$\begin{aligned} f_1(\mu) &= p(\mu), \\ f_2(\mu) &= p[p(\mu)], \\ f_3(\mu) &= p\{p[p(\mu)]\}. \end{aligned} \quad (31)$$

The step function is then:

$$s(\mu) = \frac{1}{2}[1 - f_3(\mu)] \quad (32)$$

making sure that the shift in gauge origin is normalized.

If $d(\vec{r})$ is a constant in Eq. (25), the single origin method is obtained. Keith and Bader, as well as many others have shown the inadequacies of the single origin method, and it is mentioned here only for the sake of completeness. The use of a separate nuclear centered gauge origin for each atom in a molecule is termed the method of Individual Gauges for Atoms in Molecules (IGAIM).¹⁹ The IGAIM method gives results essentially identical to the CSGT method and therefore only the later will be presented here.

III. CALCULATIONS

The above mentioned GIAO and CSGT methods have been implemented into GAUSSIAN 94²³ and all calculations were performed using this program. GIAO-MP2 chemical shifts are from Ref. 1. For comparison of DFT chemical shifts calculated here with MP2 shifts, the following $qz2p$ and $pz3d2f$ basis sets were used. The $qz2p$ basis^{1,24} which is a quadruple-zeta double polarization consists of a (11s7p2d/6s4p2d) contraction for C,N,O,F and a (6s2p/3s2p) contraction for H. The $pz3d2f$ basis set^{1,24} consists of a (13s8p3d2f/8s5p3d2f) contraction with polarization exponents taken from Ref. 25. Calculations performed with the $qz2p$ basis used geometries optimized at the MP2 level using a triple-zeta basis double polarization ($tz2p$)²⁶ basis which is a (11s6p3d/5s3p2d) for C,N,O,F

TABLE I. Convergence of Hartree-Fock GIAO and CSGT isotropic absolute shielding constants (σ , in ppm) with respect to basis set.^c

Molecule/Atom ^b	6-31G*		6-311+G(2d,p)		qz2p		pz3d2f		Expt. ^c
	GIAO	CSGT	GIAO	CSGT	GIAO	CSGT	GIAO	CSGT	
TMS									
C	195.1	190.8	188.5	188.6	188.0	186.9	187.5	188.0	188.1
Si	461.1	387.6	394.1	394.9	389.4	389.4	392.5	393.2	
CH ₄									
C	199.1	191.8	194.2	193.2	193.6	191.6	193.1	192.6	195.1
[1.1.1.]propellane (C ₅ H ₆)									
C _{me}	131.0	126.8	120.1	120.9	117.9	118.1	116.7	116.7	
C _b	204.7	189.1	197.6	198.4	197.2	196.2	196.2	195.9	
phenonium ion (C ₈ H ₉ ⁺)									
C1	148.7	145.5	136.8	137.6	134.7	134.7	133.7	133.6	
C2	21.4	16.4	4.0	4.3	-0.2	0.0	-2.7	-2.7	
C3	73.3	66.5	59.0	59.5	55.8	55.6	54.3	54.2	
C4	31.0	26.4	15.0	15.3	11.0	11.1	8.5	8.6	
C5	153.6	149.7	144.3	144.3	142.2	142.0	141.4	141.3	
CH ₃ NH ₂									
C	170.9	166.3	162.9	162.1	161.7	159.8	160.6	160.3	158.3
N	254.5	230.9	247.4	242.7	246.6	241.8	247.1	245.1	
CH ₃ F									
C	135.2	128.9	126.2	126.4	124.2	122.8	123.1	122.9	116.8
F	485.3	443.7	482.7	478.2	483.7	471.5	483.2	480.2	
CO									
C	-2.8	-10.1	-26.3	-25.0	-30.9	-31.3	-31.1	-31.2	1.0
O	-60.6	-74.0	-92.0	-90.1	-98.5	-99.9	-99.0	-99.2	-42.3

^aB3LYP/6-31G* optimized geometries. Basis sets are described in the text.

^bFor [1.1.1.]propellane, C_{me} refers to a methylene carbon while C_b refers to a bridgehead carbon. For phenonium ion, the atom labels are defined in Ref. 14.

^cExperimental ¹³C shifts are from Ref. 34 while ¹⁷O shifts are from Ref. 35.

and a (5s3p/3s2p) for H. Geometries obtained at this level of theory agree well with experiment.¹ All other calculations, with the exception of taxol, were performed at geometries optimized at the B3LYP/6-31G* level of theory. Geometries obtained at this level of theory are at least as good, and in several cases better, than those obtained at the MP2/tz2p level.²⁷

The exchange-correlation functionals considered in this work are defined as follows: The LSDA (Local Spin Density Approximation) uses Slater exchange^{16,28} and the VWN correlation functional.²⁹ BLYP uses the Becke exchange functional³⁰ and the LYP correlation functional.³¹ BPW91 uses the Becke exchange functional³⁰ and Perdew and Wang's 1991 gradient-corrected correlation functional.³² The B3PW91 functional is Becke's three parameter hybrid functional³³

$$A * E_X^{\text{Slater}} + (1 - A) * E_X^{\text{HF}} + B * \Delta E_X^{\text{Becke}} + E_C^{\text{PW91(local)}} + C * \Delta E_C^{\text{PW91(non-local)}} \quad (33)$$

with the non-local correlation provided by the Perdew 91 expression.³² The constants A , B , C , where $A=0.20$, $B=0.72$ and $C=0.81$, are those determined by Becke.³³ The

B3LYP hybrid functional,²³ which is a slight variation of Becke's three-parameter functional above, has the form

$$A * E_X^{\text{Slater}} + (1 - A) * E_X^{\text{HF}} + B * \Delta E_X^{\text{Becke}} + C * E_C^{\text{LYP}} + (1 - C) * E_C^{\text{VWN}} \quad (34)$$

where the constants A , B , C are again those determined by Becke.³³

IV. RESULTS

The convergence of the GIAO and CSGT methods with respect to basis set is demonstrated in Table I for absolute shielding constants calculated at the Hartree-Fock level of theory. The shielding constants are found to converge to the same value at sufficiently large basis sets, however, GIAO shielding constants are found to converge faster and more smoothly with respect to basis set size than those determined using the CSGT method, especially for nuclei other than carbon. This same behavior is exhibited for shielding constants calculated at the DFT level of theory. Given the similarity of shielding constants determined using either of these methods, only GIAO results will be presented from this point on.

TABLE II. Comparison of GIAO chemical shifts (δ , in ppm) calculated at the Hartree-Fock, DFT and MP2 levels of theory.^a

Molecule ^b	Nucleus	HF	LSDA	BPW91	BLYP	B3PW91	B3LYP	MP2 ^c	Expt. ^d
C ₂ H ₆	C	11.7	17.0	16.1	17.8	14.8	16.0	13.5	14.2
C ₂ H ₄	C	135.8	151.4	139.6	140.4	140.4	140.9	130.3	130.6
C ₂ H ₂	C	81.8	93.7	82.4	81.8	83.9	83.3	78.2	77.9
CH ₂ CCH ₂	C	81.7	90.5	84.5	84.5	85.2	85.1	80.6	79.9
	C	240.0	246.7	235.0	239.2	238.0	241.3	227.5	224.0
C ₆ H ₆	C	140.7	152.0	141.8	143.8	143.0	144.4	137.5	137.9
HCN	C	127.6	130.7	119.6	118.8	123.2	122.4	114.2	113.0
	N	318.6	326.3	306.2	308.4	311.8	313.4	275.2	284.9
CH ₃ NH ₂	C	31.9	42.6	40.1	42.2	38.0	39.5	36.6	36.8
	N	12.0	21.4	21.8	26.1	18.8	21.9	15.0	
CH ₃ CN	C	4.8	11.4	10.3	10.4	9.2	9.2	7.9	7.4
	C	135.1	139.0	129.1	129.7	131.9	132.2	125.4	121.3
	N	309.2	310.8	295.0	295.7	300.4	301.0	263.0	272.6
N ₂	N	391.3	370.9	355.3	356.3	364.9	365.7	321.1	326.1
NNO	N	210.8	183.5	174.0	175.6	183.3	184.7	141.1	165.0
	N	310.8	274.4	263.4	269.0	274.6	278.9	242.4	253.2
	O	177.7	172.3	169.8	169.7	173.3	173.0	138.6	143.4
CH ₃ OH	C	52.0	67.6	63.2	65.5	60.7	62.2	59.3	58.5
	O	-12.1	2.2	6.1	10.9	0.8	4.1	-5.8	
CO ₂	C	147.9	146.5	138.2	139.6	141.7	142.7	138.0	136.6
	O	112.1	129.0	120.0	118.3	120.3	118.8	103.8	100.6
CH ₂ O	C	204.9	234.7	214.4	215.1	214.6	215.0	194.8	
	O	788.1	841.5	778.0	784.5	790.8	795.5	686.7	
CH ₃ COCH ₃	C	32.2	44.9	39.7	40.6	38.5	39.2	37.0	37.1
	C	218.9	234.5	221.7	224.9	223.0	225.3	207.3	208.2
	O	667.4	707.8	676.5	676.3	684.5	683.8	624.6	
CO	C	224.9	217.6	204.9	204.8	211.4	211.3	190.4	194.1
	O	421.9	426.0	408.7	407.7	414.6	413.5	392.2	386.3
CH ₃ F	C	71.2	90.5	84.1	86.3	81.5	83.0	79.7	78.3
CF ₄	C	116.5	154.5	146.3	149.2	141.0	143.1	137.1	130.6
Absolute shielding constants for reference molecules									
CH ₄	C	195.7	193.7	190.1	187.5	191.8	189.6	201.5	195.1
NH ₃	N	262.6	266.1	260.2	259.2	261.3	260.3	276.2	264.5
H ₂ O	O	326.9	332.3	325.3	324.8	326.4	325.7	344.8	344.0

^aAll calculations performed using the $qz2p$ basis set with MP2/ $tz2p$ optimized geometries (see the text).

^bAtom order is from left to right.

^cGIAO-MP2 results from Ref. 1.

^dExperimental ¹³C values taken from Ref. 34, ¹⁵N values from Ref. 36 and ¹⁷O values from Ref. 35.

Chemical shifts, as opposed to absolute shielding constants are the primary focus of this paper as the former are measured with high accuracy in chemical applications of NMR spectroscopy. In addition, calculated chemical shifts are in better agreement with experiment as relative differences are better represented.

A. Comparison of DFT and MP2 chemical shifts

GIAO isotropic ¹³C, ¹⁵N, and ¹⁷O chemical shifts are given in Table II for several molecules obtained at the Hartree-Fock, DFT and MP2 levels of theory, using the $qz2p$ basis and MP2/ $tz2p$ optimized geometries. Chemical

TABLE III. Statistical data for ^{13}C and ^{15}N chemical shifts calculated at the Hartree-Fock, DFT and MP2 levels of theory.^a

	HF	LSDA	BPW91	BLYP	B3PW91	B3LYP	MP2 ^b
^{13}C :							
RMS error	11.5	16.1	7.7	9.2	8.7	9.5	2.3
mean error	4.0	14.4	6.5	7.8	7.0	7.9	0.8
mean absolute error	9.0	14.4	6.5	7.8	7.0	7.9	1.6
maximum error	30.8	26.3	15.7	18.6	17.3	17.3	6.5
standard deviation	4.1	15.4	11.0	4.4	5.0	5.3	9.2
absolute standard deviation	9.3	15.4	11.0	4.4	5.0	5.3	9.2
^{15}N :							
RMS error	49.3	34.6	20.0	21.7	27.5	29.1	13.4
mean error	47.8	32.8	18.4	20.6	26.6	28.4	-11.8
mean absolute error	47.8	32.8	18.4	20.6	26.6	28.4	11.8
maximum error	65.2	44.8	29.2	30.2	38.8	39.6	-23.9
standard deviation	53.4	21.5	20.2	9.0	10.1	8.1	45.5
absolute standard deviation	53.4	21.5	20.2	9.0	10.1	8.1	19.9

^aStatistical data obtained from the molecules in Table II. All calculations performed using the GIAO method, $qz2p$ basis set, and MP2/ $tz2p$ optimized geometries. ^{13}C shifts relative to CH_4 and ^{15}N shifts relative to NH_3 . Errors are with respect to experiment and reported in ppm.

^bMP2 chemical shift results taken from Ref. 1.

shifts obtained using the LSDA, BPW91, BLYP, B3PW91 and B3LYP functionals are reported. In this table, ^{13}C values are relative to CH_4 , ^{15}N values are relative to NH_3 and ^{17}O values are relative to H_2O . Note that CH_4 , as opposed to TMS, the normal standard, is used as the reference for ^{13}C shifts in order to compare directly with the MP2 results of Gauss.¹ In all cases, although more computationally demanding, MP2 predicts chemical shifts which are closer to experiment than those obtained using either Hartree-Fock or any of the DFT functionals.

Statistical measures including the RMS error, mean error, mean absolute error, maximum error and standard deviation with respect to experiment are reported in Table III for the calculated ^{13}C and ^{15}N chemical shifts. Statistical data are not reported for ^{17}O due to the limited number of experimental values. The DFT functionals consistently predict chemical shifts that are too deshielded as compared to ex-

periment using a basis set which is sufficient to predict accurate MP2 chemical shifts. With the exception of LSDA, the DFT functionals statistically provide an improvement over Hartree-Fock as judged by the RMS error. The RMS error for ^{13}C shifts is nearly the same for each of the gradient-corrected functionals and is on average 3 ppm smaller than that for Hartree-Fock. The RMS error for ^{15}N shifts calculated using the gradient-corrected functionals ranges over 9 ppm but is on average, 25 ppm smaller than the Hartree-Fock RMS error.

^{13}C chemical shifts obtained using the gradient-corrected DFT functionals are in closer agreement with experiment than those obtained at the Hartree-Fock level for HCN, CH_3CN , CO_2 , methylene carbon of acetone, and CO. For the other molecules in Table II, the gradient-corrected functionals yield chemical shifts which are roughly equal, within a few ppm, to those predicted by Hartree-Fock theory. For

TABLE IV. GIAO absolute shielding constants calculated using the $pz3d2f$ basis and experimental geometries.^a

Molecule	HF	LSDA	BPW91	BLYP	B3PW91	B3LYP	MP2 ^b	Expt. ^c
CO								
C	-25.5	-23.8	-16.1	-17.7	-19.9	-21.3	10.6	3.0
O	-87.7	-91.3	-82.1	-80.7	-85.7	-84.6	-46.5	-36.7
N_2								
N	-112.4	-95.4	-87.4	-87.9	-94.3	-94.9	-41.6	-59.6
NNO ^d								
N	62.3	85.3	88.4	86.4	81.9	80.0	130.0	127
N	-34.6	-5.2	-1.2	-6.8	-9.1	-13.6	30.3	22
O	174.1	176.7	171.8	172.5	171.2	171.6	216.2	200

^aFor CO, $r(\text{CO})=1.1283\text{\AA}$, for N_2 , $r(\text{NN})=1.0977\text{\AA}$, for NNO, $r(\text{NN})=1.1282\text{\AA}$ and $r(\text{NO})=1.1843\text{\AA}$.

^bGIAO-MP2 results from Ref. 1.

^cExperimental ^{13}C values taken from Ref. 34, ^{15}N values from Ref. 36 and ^{17}O values from Ref. 35.

^dAtom ordering is from left to right.

TABLE V. Isotropic chemical shifts (δ , in ppm).^a

Molecule	Nucleus ^b	6-31G*		6-311++G(2d,p)		Expt. ^c
		HF	B3LYP	HF	B3LYP	
C ₂ H ₆	C	4.6	3.3	5.6	4.0	7.2
C ₂ H ₄	C	116.6	110.0	125.1	124.0	123.6
C ₂ H ₂	C	62.3	54.9	71.5	67.1	70.9
CH ₂ CCH ₂	C	69.1	64.2	72.8	70.1	72.9
	C	226.1	196.4	227.0	222.0	217.4
cyclopropane						
C ₃ H ₆	C	-6.7	-5.5	-8.1	-6.7	-4.0
bicyclobutane						
C ₄ H ₆	C _{me}	22.0	23.7	23.6	26.6	32.0
	C _b	-11.0	-6.8	-11.2	-7.1	-5.7
[1.1.1.]propellane						
C ₅ H ₆	C _{me}	64.1	63.2	68.4	70.6	79.3
	C _b	-9.6	-5.8	-9.1	-3.4	4.3
C ₆ H ₆	C	122.5	115.1	131.1	128.6	130.9
phenonium ion						
C ₈ H ₉ ⁺	C1	46.4	55.5	51.7	63.8	68.8
	C2	173.7	158.9	184.5	175.4	171.8
	C3	121.8	121.9	129.5	134.9	133.4
	C4	164.1	145.8	173.5	160.5	155.4
	C5	41.5	48.2	44.2	53.7	60.7
benzonium ion						
C ₆ H ₇ ⁺	C1	35.4	40.5	38.7	47.1	52.2
	C2	184.4	172.1	195.1	189.2	186.6
	C3	121.1	123.2	128.8	136.6	136.9
	C4	186.8	163.4	196.6	178.7	178.1
HCN	C	103.5	88.7	115.8	104.7	106.0
	N	278.0	262.8	307.5	302.3	284.9
CH ₃ NH ₂	C	24.2	24.6	25.6	27.2	29.8
	N	6.3	16.3	12.9	22.8	
CH ₃ CN	C	-1.5	-4.1	-2.3	-4.1	0.4
	C	110.0	96.8	122.8	114.3	114.3
	N	274.0	256.3	299.0	290.8	272.6
N ₂	N	345.5	310.8	373.4	347.7	326.1
NNO	N	184.7	153.7	202.9	178.3	165.0
	N	268.5	230.1	295.4	267.4	253.2
	O	151.0	139.9	160.6	155.1	143.4
CH ₃ OH	C	42.8	44.4	44.6	48.8	51.5
	O	-16.5	0.8	-11.9	3.8	
CH ₂ O	C	179.9	175.5	191.7	195.4	
	O	716.6	697.0	753.2	758.4	
CH ₃ COCH ₃	C	23.2	22.3	25.2	26.0	30.1
	C	194.9	186.7	207.0	207.2	201.2
	O	633.9	627.8	654.9	666.9	
CO ₂	C	123.9	109.0	138.9	127.3	129.3
	O	94.8	93.5	107.4	112.0	100.6
CO	C	197.9	173.5	214.8	194.1	187.1
	O	383.7	365.1	413.8	402.7	386.3

TABLE V. (Continued.)

Molecule	Nucleus ^b	6-31G*		6-311+G(2d,p)		Expt. ^c
		HF	B3LYP	HF	B3LYP	
CH ₃ F	C	59.9	61.8	62.3	68.0	71.3
CF ₄	C	103.0	117.9	107.6	128.5	123.6
C ₂ B ₃ H ₅ ^d	C	82.3	90.5	88.0	99.9	103.3
	B	12.5	0.9	13.4	-0.1	3.5
Absolute shielding constants for reference molecules						
TMS	C	195.1	183.7	188.5	177.2	188.1
NH ₃	N	260.8	255.0	260.3	258.4	264.5
H ₂ O	O	323.1	316.6	321.8	320.0	344.0
B ₂ H ₆	B	106.7	93.5	101.4	83.6	

^aCalculations performed using the GIAO method and B3LYP/6-31G* optimized geometries. ¹³C shifts relative to TMS, ¹⁵N relative to NH₃, ¹⁷O relative to H₂O and ¹¹B relative to BF₃·OEt₂.

^bAtom ordering is from left to right. C_{me} and C_b refer to the methylene and bridgehead carbon, respectively. For phenonium ion and benzonium ion, the atom labels are defined in Ref. 14.

^cExperimental ¹⁵N values taken from Ref. 36 and ¹⁷O values from Ref. 35. ¹³C values are taken from Ref. 34, except for bicyclobutane and [1.1.1]propellane which are taken from Ref. 37, phenonium ion from Ref. 38, benzonium ion from Ref. 39 and C₂B₃H₅ from Ref. 40. ¹¹B value taken from Ref. 15.

^dShifts for ¹¹B calculated relative to B₂H₆ which has δ_{expt} 16.6 ppm vs BF₃·OEt₂.

¹⁵N shifts, the gradient-corrected DFT functionals provide an improvement over Hartree-Fock for each of the four molecules studied (HCN, CH₃CN, N₂ and NNO). The gradient-corrected functionals provide only a 5-8 ppm improvement over Hartree-Fock for ¹⁷O shifts in NNO, and CO, while for CO₂ these functionals predict shifts which are 7-8 ppm further from experiment than those predicted by Hartree-Fock theory. These are relatively small variations considering that the calculated shifts differ from experiment by roughly 20-35 ppm.

Absolute shielding constants for CO, N₂ and NNO, obtained using the large *pz3d2f* basis set and experimental geometries, are presented in Table IV. Gauss¹ has previously demonstrated that electron correlation effects are significant in these systems. It can be seen that the gradient-corrected DFT functionals provide only a small improvement over Hartree-Fock even at this very large basis set.

B. Hartree-Fock and B3LYP chemical shifts

In order to predict accurate NMR chemical shifts for large molecules, especially for ¹³C, it is necessary to access the accuracy of the available methods using lower levels of theory. Thus, a method is desired which will produce accurate chemical shifts at a reasonable cost.

The results in Tables II and III indicate that the gradient-corrected functionals predict chemical shifts with similar accuracy. Since the B3LYP hybrid functional has yielded excellent results for other chemical properties,^{12,13,27} this functional is chosen for closer investigation.

Hartree-Fock and B3LYP ¹³C, ¹⁵N and ¹⁷O chemical shifts, determined using 6-31G* and 6-311+G(2d,2p) basis sets, are presented in Table V. In addition to the molecules in Table II, Table V includes bicyclobutane, [1.1.1]propellane, phenonium ion, benzonium ion and C₂B₃H₅. Schleyer and

co-workers^{14,15,40} have studied these last three molecules and have concluded that MP2 is required in order to predict ¹³C and ¹¹B chemical shifts that are in good agreement with experiment. We have included these systems as a rigorous test.

In Table V ¹³C shifts are relative to TMS, ¹⁵N shifts are relative to NH₃ and ¹⁷O shifts are relative to H₂O. The ¹¹B chemical shift in C₂B₃H₅ is calculated relative to B₂H₆ with 16.6 ppm added so as to be compared to the ¹¹B experimental standard BF₃·OEt₂.⁴¹ Statistical data for the calculated ¹³C and ¹⁵N chemical shifts are reported in Table VI.

The Hartree-Fock and B3LYP 6-31G* levels of theory predict ¹³C chemical shifts with comparable accuracy. The RMS error for Hartree-Fock is 11.1 ppm for this range of molecules while for B3LYP it is 12.5 ppm. B3LYP predicts ¹³C shifts which are, in general, too deshielded, while Hartree-Fock makes errors in both directions.

¹³C chemical shifts obtained using the B3LYP functional at the larger 6-311+G(2d,p) basis have an RMS error of 4.2 ppm, compared to 11.1 ppm for Hartree-Fock at the same basis. For phenonium ion and benzonium ion, B3LYP/6-311+G(2d,p) predicted ¹³C chemical shifts are much closer to experiment than those obtained using Hartree-Fock theory at this same basis. The RMS errors for the calculated ¹³C chemical shifts in phenonium ion are 4.8 ppm and 14.6 ppm for B3LYP and Hartree-Fock, respectively. For benzonium ion, the RMS errors are 12.9 ppm for Hartree-Fock and only 2.9 ppm for B3LYP. The B3LYP/6-311+G(2d,p) level of theory also provides a significant improvement over Hartree-Fock in predicting the ¹³C and ¹¹B chemical shifts in C₂B₃H₅. The ¹³C shift differs from experiment by 15.3 ppm at the Hartree-Fock level of theory, while it differs by only 3.4 ppm using B3LYP. Similarly, the ¹¹B shift differs from experiment by 9.9 ppm and 3.4 ppm for Hartree-Fock and B3LYP, respectively.

TABLE VI. Statistical data for ^{13}C and ^{15}N chemical shifts calculated at the Hartree-Fock and B3LYP levels of theory.^a

	6-31-G*		6-311+G(2d,p)	
	HF	B3LYP	HF	B3LYP
^{13}C :				
RMS error	11.1	12.5	11.1	4.2
mean error	-6.9	-11.4	-1.0	-1.3
mean absolute error	9.3	11.4	9.2	3.6
maximum error	-22.4	-21.0	27.7	-8.4
standard deviation	7.0	9.9	11.7	11.3
absolute standard deviation	9.4	20.6	22.6	12.2
^{15}N :				
RMS error	14.5	18.2	36.5	17.2
mean error	9.8	-17.6	35.3	16.9
mean absolute error	12.5	17.6	35.3	16.9
maximum error	19.7	-23.1	47.3	21.6
standard deviation	11.0	32.9	59.4	23.1
absolute standard deviation	14.0	14.8	59.4	23.1

^aStatistical data obtained from the molecules in Table V. All calculations performed using the GIAO method and B3LYP/6-31G* optimized geometries. ^{13}C shifts relative to TMS and ^{15}N shifts relative to NH_3 . Errors are with respect to experiment and reported in ppm.

^{15}N chemical shifts calculated using the Hartree-Fock 6-31G* level of theory are closer to experiment than those determined using B3LYP at this same basis. This is due to a cancellation of errors as Hartree-Fock shifts obtained using the larger 6-311+G(2d,p) basis show a poorer agreement with experiment. B3LYP does not provide an improvement over Hartree-Fock at the smaller basis set, but does yield an improvement using the larger basis set.

Experimental ^{17}O chemical shifts are only available for three of the molecules studied here, namely NNO, CO_2 and CO. The predicted shifts are found to deviate significantly from experiment at both the Hartree-Fock and B3LYP levels of theory.

Statistical data for ^{13}C and ^{15}N chemical shifts calculated at the Hartree-Fock 3-21G* and STO-3G basis sets, for the molecules in Table V, are reported in Table VII. Hartree-Fock ^{13}C chemical shifts predicted using the STO-3G basis have an RMS error of 18.4 ppm as compared to the value of 11.1 ppm which is obtained for the larger 6-31G* and 6-311+G(2d,p) basis sets. In addition, the STO-3G basis yields a maximum error which is more than twice as large as that obtained using the larger basis sets. The Hartree-Fock 3-21G* level of theory predicts ^{13}C shifts with an RMS error similar to the larger basis sets, but with a slightly larger standard deviation.

C. Absolute shielding constants and shielding anisotropies

Statistical data for absolute shielding constants calculated using the 6-31G* and 6-311+G(2d,p) basis sets, at both the Hartree-Fock and B3LYP levels of theory, are reported in Table VIII. The results for phenonium ion, benzonium ion, $\text{C}_2\text{B}_3\text{H}_5$, bicyclobutane and [1.1.1]propellane are not included since only relative shifts have been measured for these molecules. ^{13}C and ^{15}N absolute shielding constants

determined using the B3LYP functional at the 6-31G* basis are predicted to be too deshielded as compared to experiment, while B3LYP at the larger 6-311+G(2d,p) basis predicts shielding constants which are too shielded.

The shielding anisotropy $\Delta\sigma$, which is defined as

$$\Delta\sigma = \sigma_3 - \frac{1}{2}[\sigma_2 + \sigma_1], \quad (35)$$

where $\sigma_1 < \sigma_2 < \sigma_3$ are the eigenvalues of the symmetrized shielding tensor, is an indication of the quality of the shielding tensor. Absolute shielding anisotropies are given in Table IX and exhibit the same behavior as do the absolute shielding constants.

TABLE VII. Statistical data for ^{13}C and ^{15}N chemical shifts calculated at the Hartree-Fock level of theory using small basis sets.^a

	STO-3G	3-21G*
^{13}C :		
RMS error	18.4	12.6
mean error	-10.5	-9.3
mean absolute error	15.1	10.5
maximum error	-55.6	-22.3
standard deviation	8.7	9.0
absolute standard deviation	26.2	12.7
^{15}N :		
RMS error	36.1	33.1
mean error	-22.5	26.1
mean absolute error	34.7	26.1
maximum error	-47.7	54.2
standard deviation	58.9	10.8
absolute standard deviation	24.6	10.8

^aStatistical data obtained from the molecules listed in Table V. All calculations performed using the GIAO method and B3LYP/6-31G* optimized geometries. ^{13}C shifts relative to TMS and ^{15}N shifts relative to NH_3 . Errors are with respect to experiment and reported in ppm.

TABLE VIII. Statistical data for ^{13}C and ^{15}N absolute shielding constants calculated at the Hartree-Fock and B3LYP levels of theory.^a

	6-31G*		6-311+G(2d,p)	
	HF	B3LYP	HF	B3LYP
^{13}C :				
RMS error	14.3	9.3	9.6	11.0
mean error	13.0	7.5	-1.2	-10.3
mean absolute error	13.5	7.5	7.0	10.3
maximum error	27.6	16.6	-27.3	-17.9
standard deviation	13.4	8.4	10.6	13.6
absolute standard deviation	13.9	8.4	5.7	15.4
^{15}N :				
RMS error	17.2	9.2	40.6	23.2
mean error	-13.5	8.1	-39.5	-23.0
mean absolute error	14.8	8.1	39.5	23.0
maximum error	-23.4	13.6	-51.5	-27.7
standard deviation	15.1	26.9	53.4	21.2
absolute standard deviation	16.5	26.9	35.5	70.6

^aStatistical data obtained using the molecules listed in Table II. All calculations performed using the GIAO method and B3LYP/6-31G* optimized geometries.

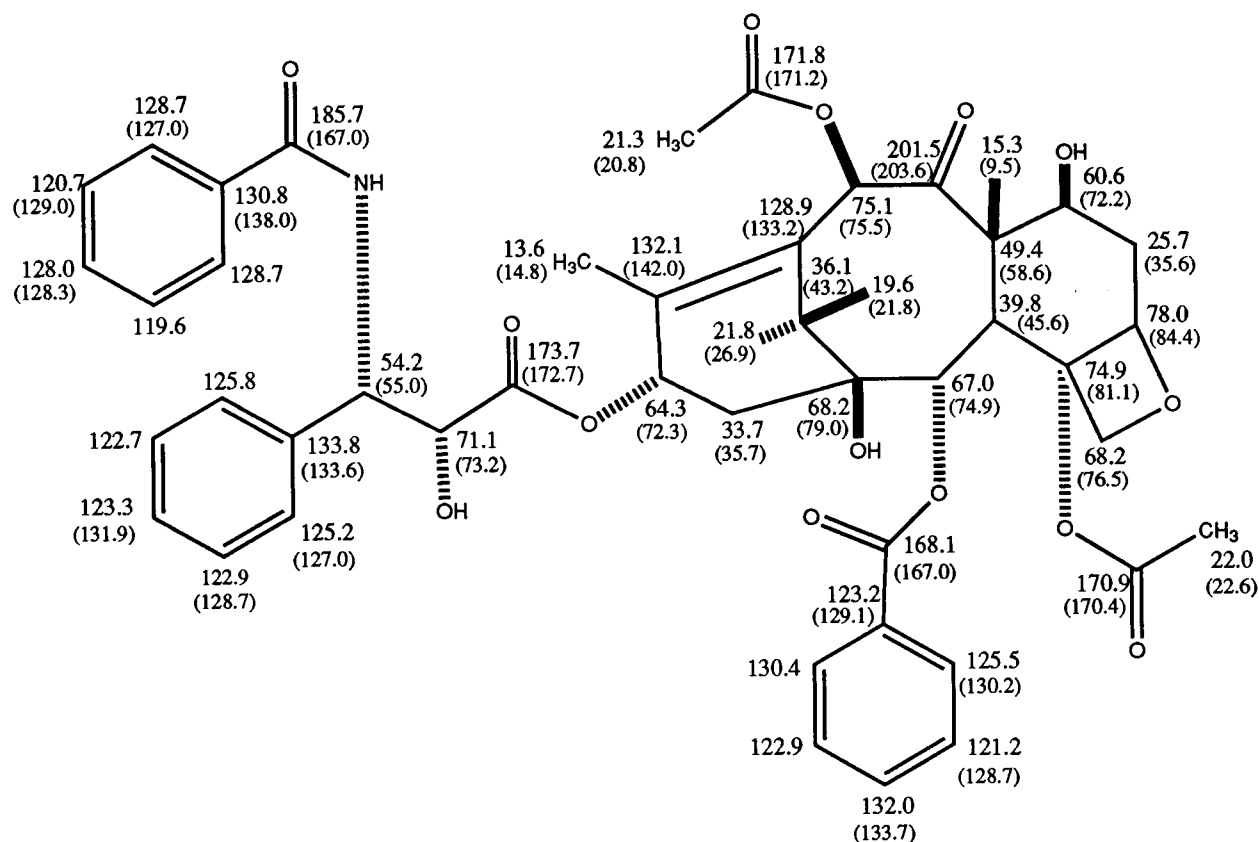


FIG. 1. Schematic diagram of taxol ($\text{C}_{47}\text{H}_{51}\text{NO}_{14}$) containing calculated and experimental (in parenthesis) ^{13}C chemical shifts relative to TMS. Calculated chemical shifts were obtained using the GIAO method at the Hartree-Fock 6-31G* level of theory and STO-3G optimized geometries. The calculated ^{13}C absolute shielding of TMS at this level of theory is 198.3 ppm. Experimental values are from Ref. 42.

TABLE IX. Hartree-Fock and B3LYP shielding anisotropies ($\Delta\sigma$, in ppm).^a

Molecule	Atom	6-31G*		6-311+G(2d,p)		Expt. ^b
		HF	B3LYP	HF	B3LYP	
CO ₂	C	316.7	314.9	349.2	352.9	335
	O	278.9	286.0	300.4	309.9	
CO	C	410.4	392.9	445.5	434.1	406.1 ± 1.4
	O	705.9	687.0	753.7	739.7	676.1 ± 26
NH ₃	N	17.4	19.3	18.2	22.2	20.0
N ₂	N	634.2	591.9	677.3	643.2	601.3

^aCalculations performed using the GIAO method and B3LYP/6-31G* optimized geometries.

^bValue derived from spin rotation constant and calculated diamagnetic part. Values cited from Refs. 6 and 11.

D. Application to large molecules: taxol

The results in Table V and Table VI indicate that ¹³C chemical shifts calculated at the Hartree-Fock 6-311+G(2d,p) level of theory are not much better, on average, than those predicted at the smaller 6-31G* basis, especially for molecules where electron correlation effects are less significant. In addition, B3LYP at the smaller basis predicts ¹³C shifts with essentially the same accuracy as does Hartree-Fock. These results suggest that the Hartree-Fock 6-31G* level of theory is sufficient to obtain accurate ¹³C chemical shifts for very large molecules where the larger B3LYP/6-311+G(2d,p) calculation is prohibitively expensive. The feasibility of this approach is demonstrated for the taxol molecule (C₄₇H₅₁NO₁₄).

A schematic diagram of the taxol molecule is shown in Fig. 1 along with the calculated and experimental ¹³C chemical shifts relative to TMS. The calculated values for taxol and TMS were obtained using the GIAO method at the Hartree-Fock 6-31G* level of theory and STO-3G optimized geometries. The statistical data for the calculated ¹³C shifts are presented in Table X.⁴³ The RMS error, with respect to experiment, is 6.4 ppm while the maximum error is 18.7 ppm (the next largest error is -11.6 ppm). The error of 18.7 ppm can most likely be attributed to the relatively poor description of the geometry. To our knowledge, the X-Ray crystal structure of taxol has not yet been determined. Despite this

TABLE X. Statistical data for calculated ¹³C chemical shifts in taxol (C₄₇H₅₁NO₁₄).^a

	HF/6-31G*
¹³ C:	
RMS error	6.4
mean error	-3.5
mean absolute error	5.0
maximum error	18.7
standard deviation	5.5
absolute standard deviation	10.2

^aCalculation performed using the GIAO method at the Hartree-Fock level of theory using the 6-31G* basis set (1032 basis functions) and the STO-3G optimized geometry. Data are for 41 carbon nuclei. Errors are with respect to experiment (Ref. 42) and are reported in ppm.

maximum error, the calculated ¹³C shifts appear to be of sufficient accuracy to aid in experimental peak assignments.

V. CONCLUSIONS

This implementation of the GIAO and CSGT methods at both the Hartree-Fock and DFT levels of theory incorporates analytical derivative techniques, hybrid density functionals and direct methods; therefore, allowing the prediction of NMR shielding tensors and chemical shifts for large molecules.

With the exception of LSDA, the pure and hybrid functionals at large basis sets yield chemical shifts which have a lower RMS error with respect to experiment than does Hartree-Fock. For molecules where correlation effects are significant, such as CO, N₂ and NNO, gradient-corrected DFT absolute shielding constants are closer to experiment than those obtained using Hartree-Fock theory.

The B3LYP 6-311+G(2d,p) level of theory predicts chemical shifts, which are quantitatively good, especially for ¹³C. This level of theory includes the effects of electron-correlation but is not quite as accurate as MP2 (for ¹⁵N and ¹⁷O shifts, in particular). Since B3LYP is more cost-effective than MP2, it represents a reasonable trade-off between accuracy and cost.

¹³C chemical shifts determined at the Hartree-Fock 6-31G* level of theory are of sufficient accuracy to be applicable to predicting chemical shifts for very large systems when the B3LYP/6-311+G(2d,p) level of theory is prohibitively expensive. This is demonstrated by the low RMS error of 6.4 ppm for the taxol example.

The exchange-correlation functionals used here do not include a specific magnetic field dependent term. Since the larger basis sets (*qz2p* and *pz3d2f*) predict chemical shifts that are systematically too deshielded, perhaps the inclusion of a magnetic field dependent term will further improve the results.

¹J. Gauss, *J. Chem. Phys.* **99**, 3629 (1993).

²T. A. Keith and R. F. W. Bader, *Chem. Phys. Lett.* **210**, 223 (1993).

³F. London, *J. Phys. Radium (Paris)* **8**, 397 (1937).

⁴R. Ditchfield, *Mol. Phys.* **27**, 789 (1974).

- ⁵ K. Wolinski, J. F. Hinton, and P. Pulay, *J. Am. Chem. Soc.* **112**, 8251 (1990).
- ⁶ J. Gauss and J. F. Stanton, *J. Chem. Phys.* **103**, 3561 (1995).
- ⁷ G. Vignale, M. Rasolt, and D. J. W. Geldart, *Adv. Quantum Chem.* **21**, 235 (1990).
- ⁸ V. G. Malkin, O. L. Malkina, and D. R. Salahub, *Chem. Phys. Lett.* **204**, 80 (1993); V. G. Malkin, O. L. Malkina, and M. E. Casida, *J. Am. Chem. Soc.* **116**, 5898 (1994).
- ⁹ W. Kutzelnigg, *Isr. J. Chem.* **19**, 193 (1980); W. Kutzelnigg, U. Fleischer, and M. Schindler, *NMR — Basic Principles and Progress* (Springer, Berlin, 1990), Vol. 23, p. 165.
- ¹⁰ K. Fredrich and G. Seifert, *Phys. D* **17**, 45 (1990).
- ¹¹ G. Schreckenbach and T. Ziegler, *J. Phys. Chem.* **99**, 606 (1995).
- ¹² C. W. Bauschlicher, Jr. and H. Partridge, *J. Chem. Phys.* **103**, 1788 (1995).
- ¹³ P. J. Stephens, F. J. Devlin, C. F. Chabalowski, and M. J. Frisch, *J. Phys. Chem.* **98**, 11623 (1994).
- ¹⁴ S. Sieber and P. v. R. Schleyer, *J. Am. Chem. Soc.* **115**, 6987 (1993).
- ¹⁵ P. v. R. Schleyer, J. Gauss, M. Bühl, R. Greatrex, and M. Fox, *J. Chem. Soc., Chem. Commun.* **1993**, 1766.
- ¹⁶ W. Kohn and L. J. Sham, *Phys. Rev. A* **140**, 1133 (1965).
- ¹⁷ B. G. Johnson and M. J. Frisch, *J. Chem. Phys.* **100**, 7429 (1994).
- ¹⁸ M. J. Frisch, M. Head-Gordon, and J. Pople, *Chem. Phys.* **141**, 189 (1990).
- ¹⁹ T. A. Keith and R. F. W. Bader, *Chem. Phys. Lett.* **194**, 1 (1992).
- ²⁰ T. A. Keith and R. F. W. Bader, *J. Chem. Phys.* **99**, 3669 (1993).
- ²¹ R. F. W. Bader and T. A. Keith, *J. Chem. Phys.* **99**, 3683 (1993).
- ²² A. D. Becke, *J. Chem. Phys.* **88**, 2547 (1988).
- ²³ GAUSSIAN 94, Revision C.2, M. J. Frisch, G. W. Trucks, H. B. Schlegel, P. M. W. Gill, B. G. Johnson, M. A. Robb, J. R. Cheeseman, T. Keith, G. A. Petersson, J. A. Montgomery, K. Raghavachari, M. A. Al-Laham, V. G. Zakrzewski, J. V. Ortiz, J. B. Foresman, J. Cioslowski, B. B. Stefanov, A. Nanayakkara, M. Challacombe, C. Y. Peng, P. Y. Ayala, W. Chen, M. W. Wong, J. L. Andres, E. S. Replogle, R. Gomperts, R. L. Martin, D. J. Fox, J. S. Binkley, D. J. Defrees, J. Baker, J. P. Stewart, M. Head-Gordon, C. Gonzalez, and J. A. Pople (Gaussian, Inc., Pittsburgh, PA, 1995).
- ²⁴ A. Schäfer, H. Horn, and R. Ahlrichs, *J. Chem. Phys.* **97**, 2571 (1991).
- The basis sets are available via FTP from host tchibm3.chemie.uni-karlsruhe.de (login id: anonymous).
- ²⁵ T. H. Dunning, Jr., *J. Chem. Phys.* **90**, 1007 (1989).
- ²⁶ The *sp* part of the basis set was taken from [T. H. Dunning, *J. Chem. Phys.* **53**, 2823 (1970)] using polarization exponents obtained from J. Gauss.
- ²⁷ M. W. Wong (personal communication).
- ²⁸ J. C. Slater, *Quantum Theory of Molecules and Solids. Vol. 4: The Self-Consistent Field for Molecules and Solids* (McGraw-Hill, New York, 1974).
- ²⁹ S. H. Vosko, L. Wilk, and M. Nusair, *Can. J. Phys.* **58**, 1200 (1980) (note that expression 3 of this paper is used).
- ³⁰ A. D. Becke, *Phys. Rev. A* **38**, 3098 (1988).
- ³¹ C. Lee, W. Yang, and R. G. Par, *Phys. Rev. B* **37**, 785 (1988).
- ³² J. P. Perdew and Y. Wang, *Phys. Rev. B* **45**, 13244 (1992).
- ³³ A. D. Becke, *J. Chem. Phys.* **98**, 5648 (1993).
- ³⁴ A. K. Jameson and C. J. Jameson, *Chem. Phys. Lett.* **134**, 461 (1987).
- ³⁵ R. E. Wasylshen, S. Mooibroek, and J. B. Macdonald, *J. Chem. Phys.* **81**, 1057 (1984).
- ³⁶ C. J. Jameson, A. K. Jameson, D. Oppungu, S. Wille, and P. M. Burrell, *J. Chem. Phys.* **74**, 81 (1981).
- ³⁷ A. M. Orendt, J. C. Facelli, D. M. Grant, J. Michl, F. H. Walker, W. P. Dailey, S. T. Waddell, K. B. Wiberg, M. Schindler, and W. Kutzelnigg, *Theor. Chim. Acta* **68**, 421 (1985).
- ³⁸ G. A. Olah, R. J. Spear, and D. A. Forsyth, *J. Am. Chem. Soc.* **99**, 2615 (1977).
- ³⁹ G. A. Olah, J. S. Staral, G. Asencio, G. Liang, D. A. Forsyth, and G. D. Mateescu, *J. Am. Chem. Soc.* **100**, 6299 (1978).
- ⁴⁰ M. Bühl, J. Gauss, M. Hofmann, and P. v. R. Schleyer, *J. Am. Chem. Soc.* **115**, 12385 (1993).
- ⁴¹ The $\delta^{11}\text{B}$ experimental values are reported relative to the experimental standard $\text{BF}_3 \cdot \text{OEt}_2$ which is shifted 16.6 ppm upfield from B_2H_6 .
- ⁴² D. G. I. Kingston, *Pharmac. Ther.* **52**, 1 (1991).
- ⁴³ Experimental ^{13}C shifts are only available for 41 out of the 47 carbon nuclei.